Supplementary Information for Lab on a Chip

An Ultra-Rapid Acoustic Micromixer for Synthesis of Organic Nanoparticles

M.Reza Rasouli,[a] Maryam Tabrizian,*[a,b]

[a] Biomedical Engineering Department-Faculty of Medicine, McGill University, Montreal, Quebec H3A 2B4, Canada

[b] Faculty of Dentistry, McGill University, Montreal, Quebec H3A 2B4, Canada

Bubble trapping

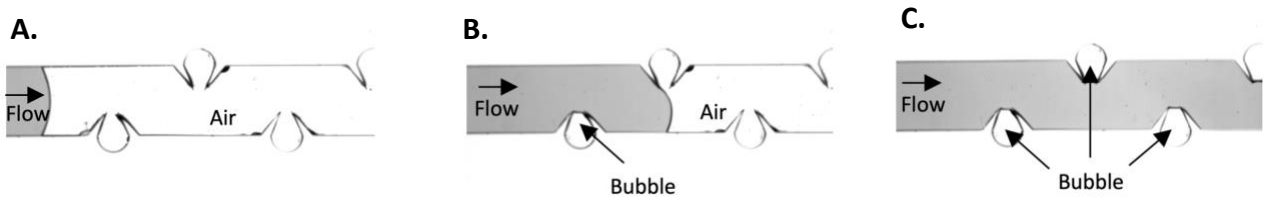

Figure S1. The channels are initially empty which means there is only air in them. When an aqueous liquid gets infused to the channel, it fills all the channel except for the sequestered volume between the slanted sharp-edges due to the surface tension, leaving a trapped bubble.

Impedance Analysis

In the majority of works related to bubble-based acoustic streaming, the pronounced frequency is attributed to the natural frequency of the bubble calculable by the Rayleigh-Plesset equation. However, the independence of this frequency from the bubble's existence in Fig. 3a and also the identical optimum frequency of different-sized bubbles in Fig. 3b which by Rayleigh-Plesset equation should be different, highlight the role of the electromechanical resonance of the piezoelectric.

Fig. S2 shows the impedance sonogram for the transducer mounted on a 1mm thick glass substrate, adjacent to the PDMS microchannels. The spectrum has a smooth behavior except at the frequency of 75.6 kHz, which is close to the optimum frequency of microstreams, where strong fluctuation in the impedance amplitude occurs.

Since the bubble's volumetric pulsation which is the dominant source of microstreaming is absent at frequencies other than the bubble's natural frequency, the most plausible explanation would be that the vibration of sharp-edges allows fluctuation of the volume sequestered between them leading to an artificial volumetric pulsation. The combination of this volumetric pulsation and translational oscillation in the bubble with amplified sharp-edges vibration due to the lower viscous resistance of the bubble creates a positive feedback phenomenon that leads to a significant increase in microstreams intensity.

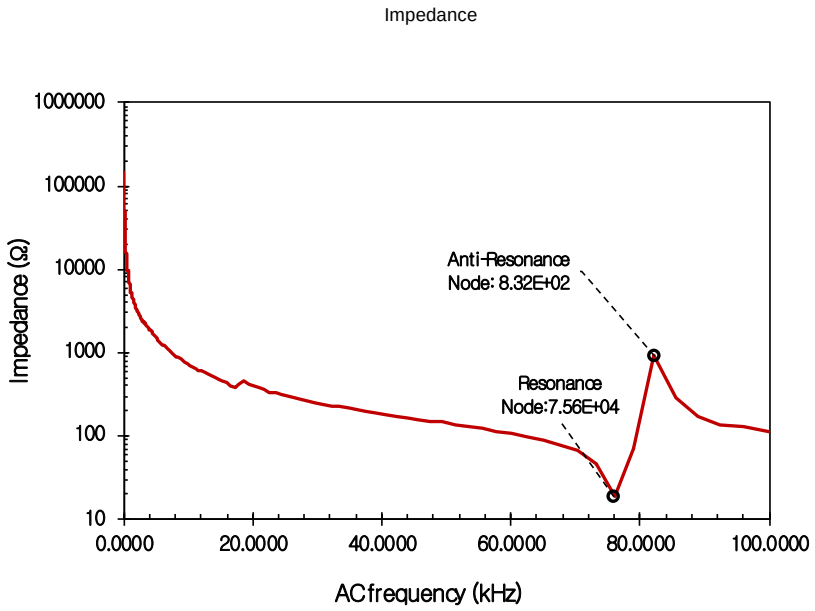

Figure S2. Sonogram of impedance and phase for piezoelectric transducer model no. 273-073, Radioshack. The resonance frequency is in line with reported optimum frequency for mixing index.

Mixing

To visualize and characterize the mixing process by the acoustic microstreams, DI water and fluorescein solution were infused simultaneously through two separate inlets with a flow rate of Q = 18 µL/min. Fig. S3A shows the laminar flow pattern of the solutions moving side by side in the direction of the channel. In the absence of the acoustic field, the advection ensued only in the direction of the laminar flow. Thus, the mixing process is purely dependent on the diffusion process which is by nature very slow and ineffective, as witnessed by the discernible interface and unmixed fluid domains. Upon excitation with an input voltage of 14 V_{PP}, the piezoelectric transducer emanates the driving acoustic pressure required for inducing closed-circular

microstreams and homogenous mixing of DI water and fluorescein (Fig. S3B). The motion momentum of acoustic microstreams prevails over the laminar flow and disrupts its parallel streamlines, including the interface of fluids.

The rotational fluid motion exponentially increases the interface of fluids by twisting and stretching it. This microscale stirring drastically accelerates the previously sluggish mixing process by increasing the interface of fluids and hence, curtailing the diffusion distance through twisting and stretching along with reciprocal advection of mass fractions between the co-flowing fluids.[1]

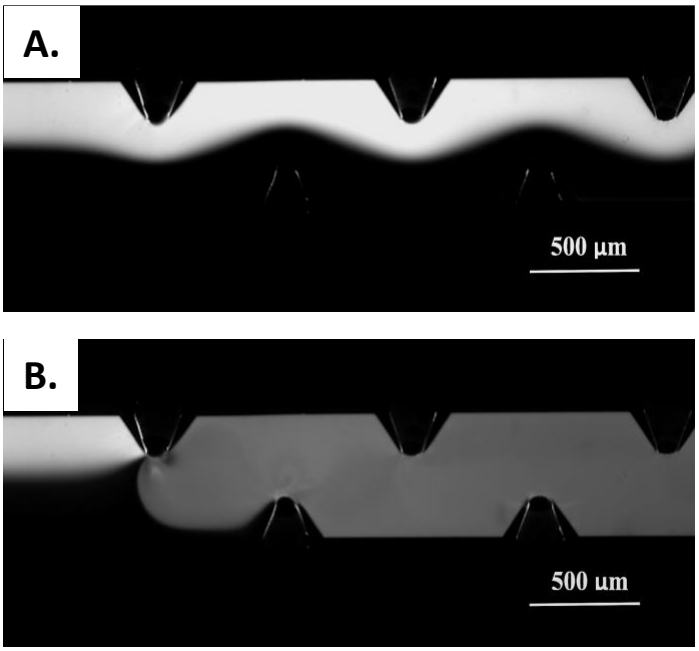

Figure S3. The concentration distribution of fluorescein and DI water in the A) absence and B) presence of acoustic mixing.

Mixing Index

To visualize and characterize the mixing process by the acoustic microstreams, DI water and fluorescein solution were infused simultaneously through two separate inlets. Mixing index was employed as the quantitative function for evaluation of the mixing quality through the width of the channel.

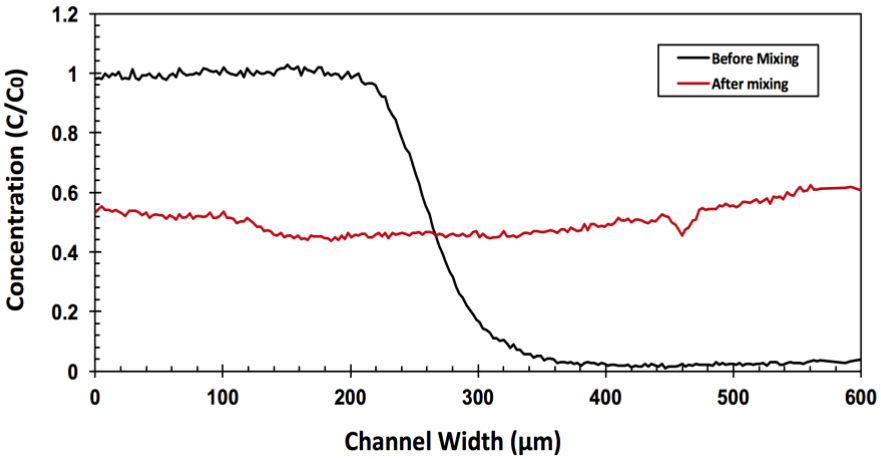

Figure S4. Concentration profile across the channel width before and after mixing by acoustic microstreams.

The variance of normalized concentrations was obtained at the reference cross-section from the gray-scale images. The mathematical form of the function is:

$$\mathrm{MI} = 1 - \sqrt{\frac{\frac{1}{N}\sum_{i=1}^{N}(c_i - \langle c \rangle)^2}{\langle c \rangle (1 - \langle c \rangle)}} \qquad \text{(S1)}$$

where N is the number of sampling elements, c_i exhibits the concentration of each mass fraction, and $\langle c \rangle$ shows the average concentration of the cross-section. For perfectly mixed solutions, the mixing index equals one, whereas for completely segregated flows the value is zero. A mixing index of 0.8 was designated as the lower threshold for adequate mixing.

For Fig. 2C, mixing index was measured at mixing distance of 2500 µm as shown in Fig S5B.

For measuring the mixing distance in Fig 4b., the horizontal length needed to reach to normalized concentration of 0.6 was measured for 10 nodes.

Variation in Voltage

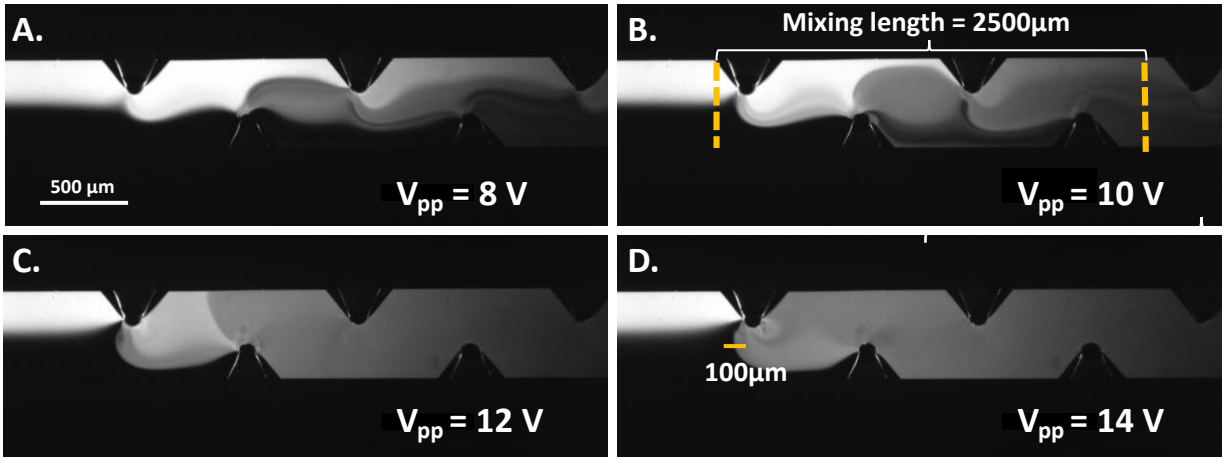

Fig S5. Mixing performance by changing the input voltage at the flow rate of 18 µL/m.

Variation in Flow Rate

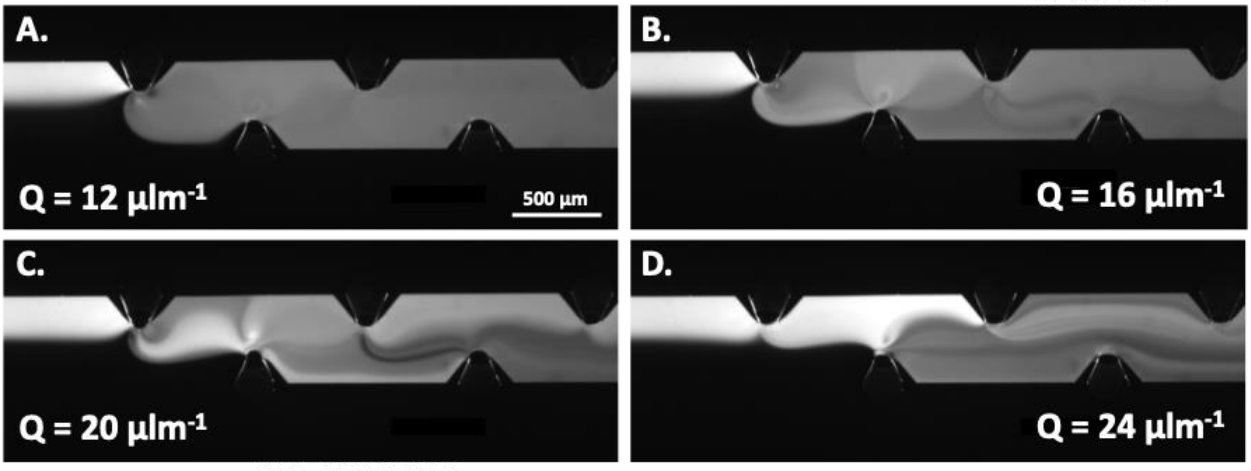

Fig S6. Mixing performance by changing the flow rate at the input voltage of 10 V_{PP}.

PLGA-PEG nanoparticle size distribution

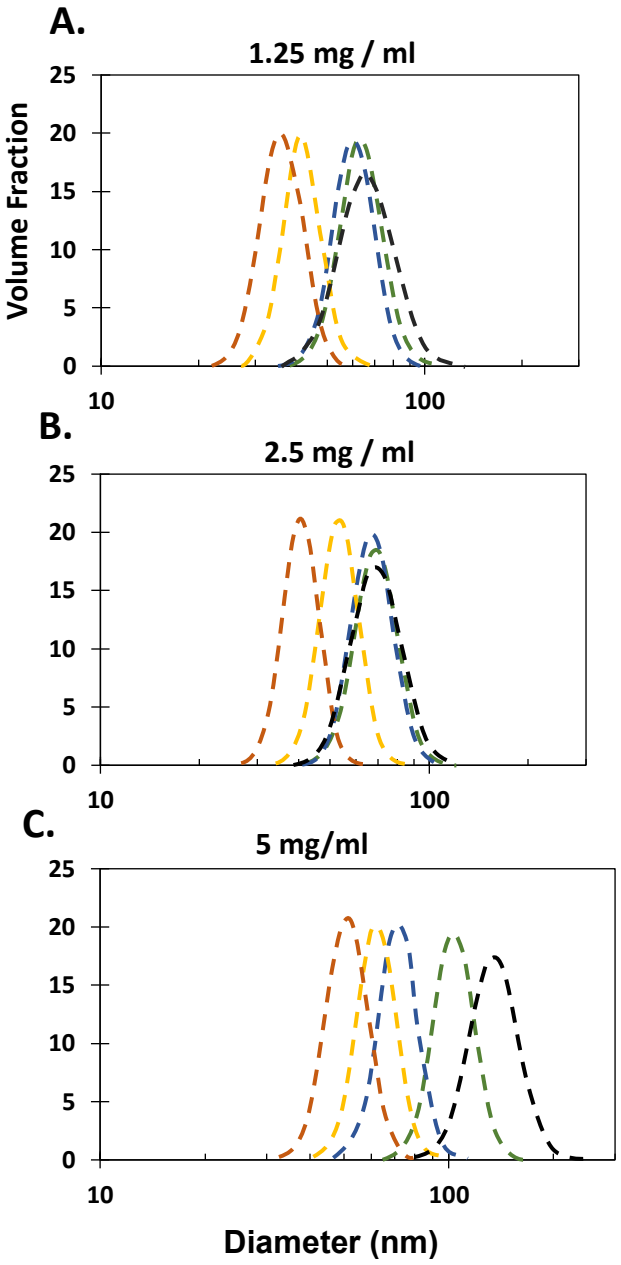

Fig S7. Size distribution of PLGA-PEG nanoparticles with precursor concentration of A) 1.25 mg/ml, B) 2.5 mg/ml and C) 5 mg/ml measured by DLS.

Liposome size distribution

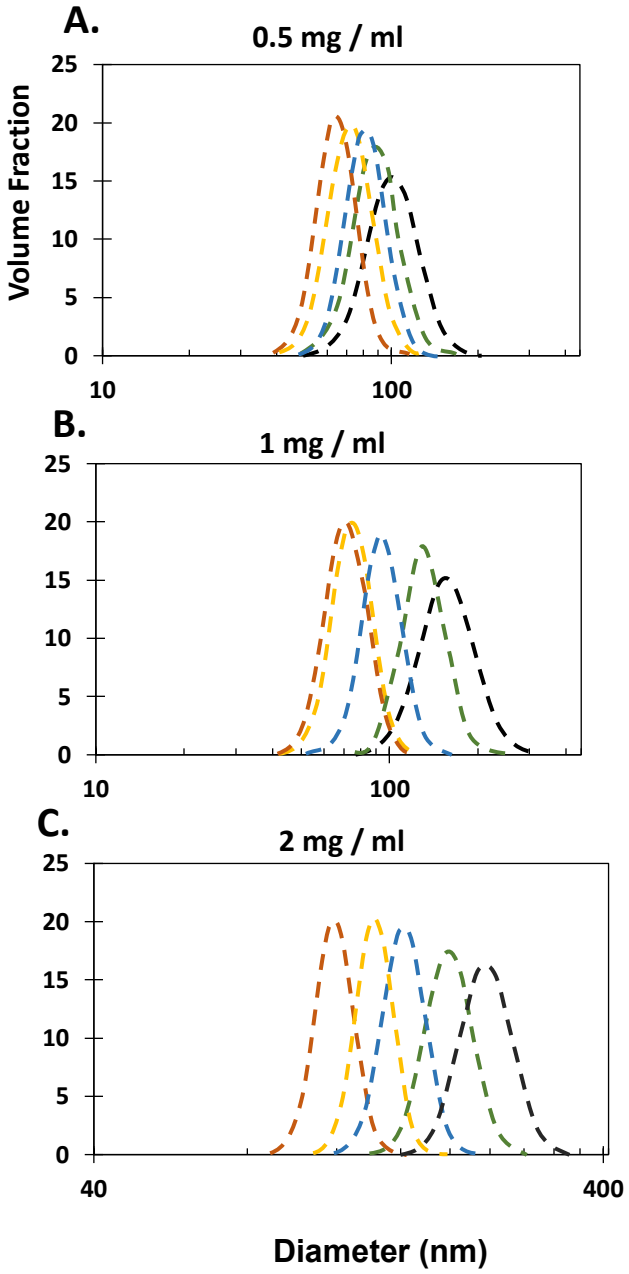

Fig S8. Size distribution of Liposomes with precursor concentration of A) 0.5 mg/ml, B) 1 mg/ml and C) 2 mg/ml measured by DLS.

Video captions.

Video S2: The 2-micron diameter polystyrene particles showing the pattern of microstreams in response to acoustic field.

Video S3: The microstream pattern shown by trajectory of 2-micron diameter polystyrene particles for a sharp-edge feature without bubble (left feature) and the integrated feature of bubble and sharp edges (right feature).

Video S4: The microstream pattern shown by trajectory of 2-micron diameter polystyrene particles for bubbles in the absence of sharp edges.

Video S5: The mixing performance of the design by variation of the input voltage at the constant flow rate of 18 μL/m.

Video S6: The mixing performance of the design by changing the flow rate at the constant input voltage of 10 Vpp.

Video S7: NTA video of liposomes produced in HFF method with dilution factor of 200.

Video S8: NTA video of liposomes produced in acoustic micromixer with dilution factor of 200.